


Experimental study on alleviating atherosclerosis through intervention of mitochondrial calcium transport and calcium-induced membrane permeability transition

Sisi Chen,¹ Jianing Wang,^{1,2} Lei Zhang,³ Hao Xia ^{1,4,5}

► Additional supplemental material is published online only. To view, please visit the journal online (<http://dx.doi.org/10.1136/jim-2020-001765>).

¹Department of Cardiology, Renmin Hospital of Wuhan University, Wuhan, Hubei, China

²Department of Cardiology, Renmin Hospital, Hubei University of Medicine, Shiyan, Hubei, China

³Department of Cardiology and Institute of Clinical Medicine, Renmin Hospital, Hubei University of Medicine, Shiyan, Hubei, China

⁴Cardiovascular Research Institute, Wuhan University, Wuhan, Hubei, China

⁵Hubei Key Laboratory of Cardiology, Wuhan, Hubei, China

Correspondence to

Dr Hao Xia, Department of Cardiology, Renmin Hospital of Wuhan University, Wuhan 430060, China; xiahao1966@163.com

Accepted 31 March 2021
Published Online First
27 April 2021



© American Federation for Medical Research 2021. No commercial re-use. See rights and permissions. Published by BMJ.

To cite: Chen S, Wang J, Zhang L, et al. *J Investig Med* 2021;**69**:1156–1160.

ABSTRACT

To investigate the effort of mitochondrial calcium transport and calcium-induced membrane permeability transition in alleviating atherosclerosis. The experimental mice were divided into three groups: the control group (C57BL/6 mice with normal diet), the atherosclerosis group (apolipoprotein E-deficient (ApoE^{-/-}) mice with high-fat diet) and the mitochondrial targeting agent group (ApoE^{-/-} mouse with high-fat diet). The mean fluorescence intensity of Ca²⁺ in the atherosclerosis group is significantly higher than control group and mitochondrial targeting agent group. But the mean fluorescence intensity of Ca²⁺-ATPase is lower than other groups. The macrophage recruitment (F4/80 positive area) and the expression of tumor necrosis factor alpha, interleukin-6, pyrin domain containing protein 3, intercellular cell adhesion molecule-1, p38 mitogen-activated protein kinase and Jun kinase 1/2 phosphorylation in the atherosclerosis group are higher than other groups. Treatment with mitochondrial targeting agents reduced the levels of elevated cyt C and cleaved caspase-3 in atherosclerotic mice (p<0.05). Mitochondrial targeting agents interfere with mitochondrial calcium transport and calcium-induced membrane permeability transition, inhibit MAPK/JNK pathway activation, inhibit foam cell formation and alleviate the process of atherosclerosis.

INTRODUCTION

Atherosclerosis is the leading cause of death and disability worldwide. The endothelium is the cellophane-like membrane of the circulatory system, and its main function is to regulate the tone and wall permeability of blood vessels.¹ Endothelial cell dysfunction is related to the early stages of many cardiovascular diseases, which makes the regulation of endothelial cell function a key therapeutic target. Under normal circumstances, the function of endothelial cells depends on changes in intracellular calcium ion (Ca²⁺) concentration.² In endothelial cells, mitochondria account for 25% of cellular Ca²⁺ storage.³ It has long been determined that endothelial cells contain moderate mitochondria (endothelial mitochondria account for 2%–6%

Significance of this study

What is already known about this subject?

- Atherosclerosis is the leading cause of death and disability worldwide.
- Endothelial cell dysfunction is related to the early stages of many cardiovascular diseases, which makes the regulation of endothelial cell function a key therapeutic target.
- Endothelial cell apoptosis is a key process in the development of atherosclerosis.

What are the new findings?

- We found that mitochondrial targeting agents significantly inhibited atherosclerosis in apolipoprotein E-deficient (ApoE^{-/-}) mice fed a high-fat diet. In addition, mitochondrial targeting agents also inhibited the expression of F4/80 in ApoE^{-/-} mice.
- ASC and pyrin domain containing protein 3 (NLRP3) together lead to the lysis of procaspase-3 and the activation of caspase-3 in the form of spotted cytoplasmic aggregation.
- Mitochondrial targeting agents can inhibit the development of atherosclerosis and induce the formation of foam cells in ApoE^{-/-} mice.
- Mitochondrial targeting agent treatment reduced the levels of elevated cyt C and cleaved caspase-3 in atherosclerotic mice.

How might these results change the focus of research or clinical practice?

- Mitochondrial targeting agents inhibit the activation of the mitogen-activated protein kinase/Jun kinase pathway by suppressing mitochondrial calcium transport and calcium-induced membrane permeability change, inhibit foam cell formation and alleviate atherosclerosis.

of cytoplasmic volume), while cardiomyocytes (occupies 32% of cytoplasmic volume) and other cell types because endothelial cells have

relatively high energy requirements and glycolysis is the main source of ATP production.⁴ Endothelial cell apoptosis is a key process in the development of atherosclerosis.⁵ Due to apoptosis, endothelial cells may lose the ability to regulate lipid homeostasis, immunity and inflammation.⁶ Endothelial cell damage can destroy the integrity and barrier function of the endothelium and promote lipid deposition, leading to atherosclerosis.⁷ In addition, endothelial cell apoptosis is the cause of plaque instability because the death of endothelial cells may lead to arterial thrombosis, leading to acute coronary occlusion and sudden death.⁸ In the development of atherosclerosis, macrophages become foam cells, which initially accumulate in the vascular intima and participate in the progression of the disease.⁹ Plaques rich in foam cells are more likely to rupture, leading to thrombosis and subsequent cerebrovascular disease events.¹⁰ This article explores how to alleviate the process of atherosclerosis by intervening in mitochondrial calcium transport and calcium-induced membrane permeability transition.

MATERIALS AND METHODS

Experimental animals

C57BL/6 and C57BL/6 background *ApoE* $-/-$ mice (8 weeks old) were purchased from the Animal Research Center. A total of 24 *ApoE* $-/-$ mice were treated with or without mitochondrial targeting agent (1 mmol/L) and fed with a high-fat diet for 8 weeks. C57BL/6 mice were used as control. The hearts containing the aortic root and aortic arch were frozen in liquid nitrogen and stored at -80°C for further analysis.

Methods

Assessment of cytosolic calcium

The cells inoculated on the coverslip were washed three times with a calcium ion-containing buffer (136 μM NaCl, 5.4 μM KCl, 10 μM HEPES, 0.33 μM $\text{NaH}_2\text{PO}_4 \cdot 2\text{H}_2\text{O}$, 1 μM $\text{MgCl}_2 \cdot 6\text{H}_2\text{O}$, 1 μM glucose and 1.8 μM CaCl_2 , pH, 7.4). The cells were incubated with 5 $\mu\text{mol/L}$ Fluo-3/AM (Molecular Probes, Eugene, Oregon, USA) at 37°C for 35–45 min. After washing with calcium buffer, the cells were observed under a confocal laser scanning microscope (FV300, Olympus, Japan, excitation wavelength is 495 nm, and emission wavelength is 525 nm).

Analysis of plaque lesions

The hearts were obtained and fixed in 4% paraformaldehyde and dehydrated in sucrose. After embedding with optimal cutting temperature, the tissue was cut into 10 μm sections for histological analysis. H&E, Oil Red O and Masson staining was done to quantify the area of the lesion and staining for lipid and collagen. All experiments were performed in accordance with the manufacturer's instructions (KeyGEN BioTECH, China). Representative images were analyzed by Image Pro Plus software.

Immunohistological analysis

The sections were incubated with anti-F4/80, tumor necrosis factor alpha (TNF- α), interleukin 6 (IL-6), pyrin domain containing protein 3 (NLRP3) and intercellular cell adhesion molecule-1 (ICAM1) antibodies (Abcam, USA) at 4°C overnight. After washing with phosphate buffer saline

(PBS), the sections were incubated with secondary antibody for 1 hour and counterstained with hematoxylin. Image-Pro Plus software was used to quantify the expression of F4/80, TNF- α , IL-6, NLRP3 and ICAM1.

Western blotting assays

Cells were lysed with radio immunoprecipitation assay buffer containing protease and phosphatase inhibitors. After centrifugation, the supernatant was collected and quantified. The proteins were separated by sodium dodecyl sulfate polyacrylamide gel electrophoresis (SDS-PAGE) and transferred to nitrocellulose membrane. After blocking with 5% skimmed milk, it was treated with anti-phospho-p38 mitogen-activated protein kinase (MAPK) (Santa Cruz Biotechnology, Dallas, Texas, USA) and anti-phospho-Jun kinase 1/2 (JNK1/2) antibodies (Cell Signaling Technology, Danvers, Massachusetts, USA), followed by incubation with fluorescently labeled secondary antibodies. The western blot protein band was scanned using Odyssey Imaging System (LI-COR, Lincoln, Nebraska, USA). GAPDH (Zhongshan Golden Bridge, Beijing, China) was used as an internal control.

Real-time RT-PCR

The mouse aorta was exposed, and the surrounding tissue was carefully removed. After perfusion with saline, the aorta was removed and transferred to a Petri dish containing ice-cold PBS. In order to obtain samples from the prone and non-prone sites, the aorta was cut into two parts: the aortic arch (prone site) and the thoracic-abdominal aorta (prone site). An insulin syringe was used to quickly rinse the preparation with TRIzol reagent (Invitrogen, Carlsbad, California, USA), and the eluate was collected in a 1.5 mL test tube and was prepared for RNA extraction. The remaining aorta (medium+adventitia) was stored at -80°C until RNA extraction. According to the manufacturer's protocol, total RNA was harvested from tissues and cells using TRIzol reagent (Invitrogen). The extracted RNA was reverse transcribed into cDNA using a high-capacity cDNA reverse transcription kit (Applied Biosystems, Foster City, California, USA). Real-time PCR was performed using first-strand cDNA, and β -actin was used as an internal control to quantify the mRNA expression of phospho-p38 MAPK, phospho-JNK1/2, cyt C and caspase-3. Online supplemental table 1 shows the primer sequences in RT-PCR.

Statistical analysis

Data were expressed as mean \pm SD and analyzed using Student's *t*-test or analysis of variance test. A two-tailed $p < 0.05$ was considered statistically significant. SPSS V.22.0 (IBM SPSS, New York, USA) was used for analysis.

RESULTS

Mitochondrial targeting agents promote mitochondrial calcium transport in *ApoE* $-/-$ mice

Fluorescence intensity detection by laser confocal microscopy showed intracellular Ca^{2+} concentration. Compared with the control group, the mean fluorescence intensity of Ca^{2+} in the atherosclerosis group increased and the Ca^{2+} -ATPase decreased ($p < 0.05$). Compared with the atherosclerosis group, the mean fluorescence intensity of Ca^{2+} was

Table 1 Mitochondrial targeting agents promote calcium transport from cytoplasm to mitochondria

Group	Mean fluorescence intensity of Ca ²⁺	Ca ²⁺ -ATPase
Control	11.43±1.25	8.89±0.37
Atherosclerosis group	124.32±8.76	1.87±0.14
Mitochondrial targeting agent group	48.37±5.22	3.58±0.34
F value	13.264	12.023
P value	0.017	0.011

decreased and Ca²⁺-ATPase was increased in the mitochondrial targeting group ($p < 0.05$) (table 1).

Mitochondrial targeting agents inhibit the development of atherosclerosis in ApoE^{-/-} mice

ApoE^{-/-} mice were euthanized with or without mitochondrial targeting agents, and aortic root slices were used to quantify plaque lesions. H&E, Masson and Oil Red O staining showed that compared with the control group, the lesion area, collagen and lipid content in the atherosclerosis group were increased ($p < 0.05$), while the lesion area, collagen and lipid content in the mitochondrial targeting group were decreased ($p < 0.05$) (table 2).

Mitochondrial targeting agents reduce macrophage recruitment

Since macrophages play a key role in early atherosclerosis, we evaluated the recruitment of macrophages in plaque lesions. Compared with the control group, macrophage recruitment (F4/80 positive area) of the atherosclerosis group was increased ($p < 0.05$), and compared with the atherosclerosis group, the recruitment of macrophages (F4/80 positive area) was reduced in the mitochondrial targeting agent group ($p < 0.05$) (online supplemental table 2).

Mitochondrial targeting agents reduce the expression of proinflammatory cytokines

Atherosclerotic factors such as TNF- α , IL-6, NLRP3 and ICAM1 are involved in the development of atherosclerosis. Immunohistochemical staining of the aortic arch showed that compared with the control group, the expression of TNF- α , IL-6, NLRP3 and ICAM1 increased in the atherosclerosis group ($p < 0.05$); compared with the atherosclerosis group, the expression of TNF- α , IL-6, NLRP3 and ICAM1 decreased in the mitochondrial targeting agent group ($p < 0.05$) (figure 1 and online supplemental table 3).

Table 2 Mitochondrial targeting agent inhibits the development of atherosclerosis in ApoE^{-/-} mice

Group	Area of lesion (mm ²)	Collagen (%)	Oil Red O stain (%)
Control	0.01±0.01	3.43±0.17	6.12±0.35
Atherosclerosis group	0.27±0.04	18.25±1.26	75.43±5.16
Mitochondrial targeting agent group	0.12±0.05	8.47±0.21	26.37±2.18
F value	12.324	15.324	15.428
P value	0.011	0.012	0.015

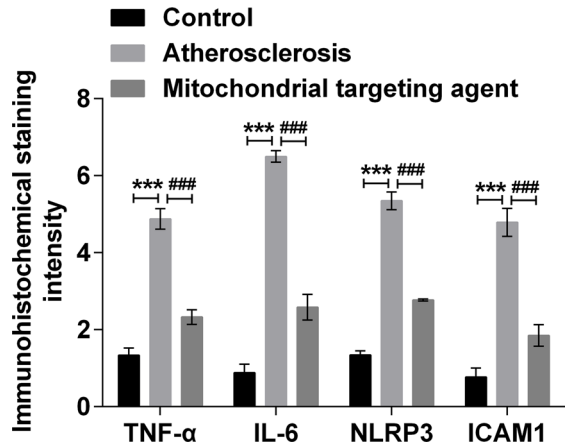


Figure 1 Immunohistochemical staining intensity of TNF- α , interleukin 6 (IL-6), NLRP3 and ICAM1 expression. *Significant difference between control and atherosclerosis group, *** $p < 0.001$. #Significant difference between atherosclerosis and mitochondrial targeting agent group, ### $p < 0.001$.

Mitochondrial targeting agents inhibit MAPK/JNK expression

The MAPK/JNK pathway is involved in lipid accumulation in macrophages. Therefore, we carried out western blotting and RT-PCR assays to further clarify the mechanism, whereby mitochondrial targeting agents inhibit foam cell formation. Our results showed that compared with the control group, the expression of p38 MAPK and JNK1/2 phosphorylation was increased in the atherosclerosis group ($p < 0.05$). Compared with the atherosclerosis group, the expression of phosphor-p38 MAPK and JNK1/2 decreased in the treatment group ($p < 0.05$). It indicates that the MAPK/JNK pathway is involved in the development of atherosclerosis mediated by mitochondrial targeting agents (figure 2, online supplemental tables 4 and 5).

Mitochondrial targeting agents inhibit mitochondrial apoptosis pathway

Since calcium is a key activator of mitochondrial apoptosis pathway, we explored whether mitochondrial targeting agents inhibit apoptosis through calcium-activated apoptosis pathway. Our results showed that, compared with the control group, the apoptotic cascade was activated after triggering calcium overload in the atherosclerosis group, as evidenced by the release of cyt C and the activation of caspase-3 ($p < 0.05$). In contrast, treatment with mitochondrial targeting agents reduced the levels of elevated cyt C and cleaved caspase-3 in atherosclerotic mice ($p < 0.05$) (figure 3 and online supplemental table 6).

DISCUSSION

Atherosclerosis is the root cause of cardiovascular disease, accounting for about 50% of deaths worldwide. It is traditionally believed that atherosclerosis is caused by impaired lipid metabolism, which is mainly manifested by elevated plasma levels of low-density lipoprotein cholesterol.¹¹ Inflammation has also become the cause of the formation of atherosclerotic plaques. According to the latest hypothesis, inflammation and lipid metabolism jointly promote

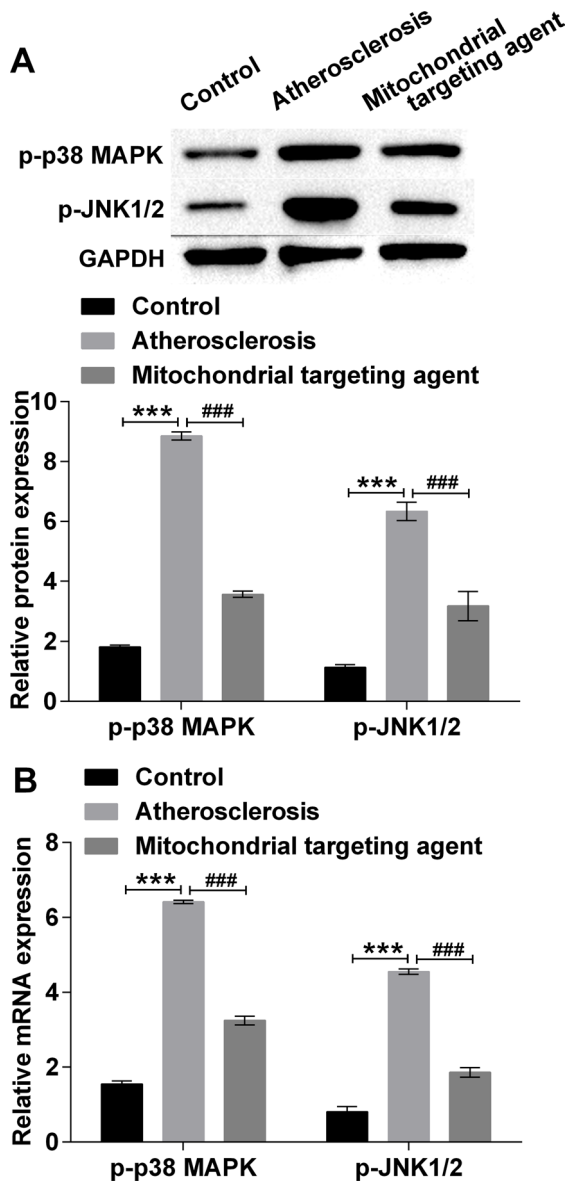


Figure 2 Western blot and RT-PCR analysis of p-p38 MAPK and p-JNK1/2 expression. (A) Protein expression levels of p-p38 MAPK and p-JNK1/2 detected by western blot. (B) mRNA expression levels of p-p38 MAPK and p-JNK1/2 detected by RT-PCR.

*Significant difference between control and atherosclerosis group, *** $p < 0.001$. #Significant difference between atherosclerosis and mitochondrial targeting agent group, ### $p < 0.001$.

the formation of atherosclerotic plaques in the arterial wall. Mitochondria have a large negative membrane potential of 180 mV, which can promote Ca^{2+} to enter mitochondria from the cytoplasmic environment. In the process of evolution, cells have acquired a complex mitochondrial Ca^{2+} transport mechanism, which controls the entry of Ca^{2+} into the mitochondrial matrix and the redistribution of Ca^{2+} in order to maintain cell function.¹² The formation of spots also requires ASC phosphorylation. MAPK and JNK are two kinases that phosphorylate ASC. Inhibition of MAPK or JNK will interfere with the formation of ASC spots but will not affect the combination of ASC and NLRP3.¹³ The formation of ASC spots is necessary for the activation of

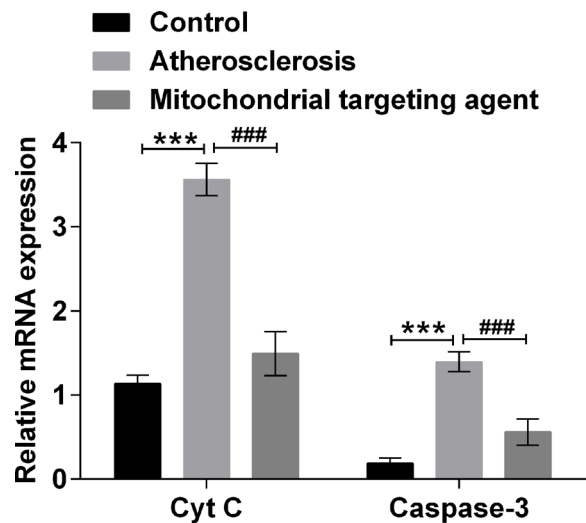


Figure 3 RT-PCR analysis of cyt C and caspase-3 expression. *Significant difference between control and atherosclerosis group, *** $p < 0.001$. #Significant difference between atherosclerosis and mitochondrial targeting agent group, ### $p < 0.001$.

inflammasomes. The necessity of ASC phosphorylation to form ASC spots indicates the mechanism of formation of inflammasome complexes: K^+ efflux, reactive oxygen species (ROS) formation, Ca^{2+} signaling, endoplasmic reticulum (ER) stress, mitochondrial dysfunction and lysosome rupture.¹⁴ These mechanisms are overlapped, and we interpret them as four mechanisms: (1) K^+ efflux, (2) ROS formation, (3) ER stress-induced mitochondrial dysfunction- Ca^{2+} signaling and (4) lysosomal rupture. There is an interaction between Ca^{2+} level and ER stress. In this way, IP2R can be adjusted to regulate the flow of Ca^{2+} out of the ER, as the fourth sensor of ER stress. In a stress-free cell state, the appropriate and necessary amount of Ca^{2+} leave the ER through IP3R. During the initial and adaptation stage of ER stress, IP3R reduces Ca^{2+} outflow. However, during prolonged ER stress beyond an adjustable level, IP3R promotes apoptosis by increasing the flow of Ca^{2+} from the ER.¹⁵ The cytoplasmic Ca^{2+} content increases, and Ca^{2+} enters the mitochondria and causes ROS production. Mitochondrial ROS leads to mtDNA oxidation, which leads to inflammasome activation. Ca^{2+} can also activate the tat-related kinase (TAK1)-JNK pathway to activate the kinase JNK, which is necessary for the formation of ASC spots. Increased extracellular Ca^{2+} can also cause activate inflammasomes.¹⁶ An increase in extracellular Ca^{2+} concentration at the site of infection and chronic inflammation was observed. Necrotic cells seem to be a resource for increased extracellular Ca^{2+} , which activates the NLRP3 inflammasome through the G protein-coupled calcium-sensitive receptor in the inositol (1,4,5)-triphosphate (PI3)/ Ca^{2+} pathway.¹⁷ We observed that compared with the control group, the mean fluorescence intensity of Ca^{2+} in the atherosclerosis group increased, and the Ca^{2+} -ATPase decreased; the lesion area, collagen and lipid content increased ($p < 0.05$). Compared with the atherosclerosis group, the mean fluorescence intensity of Ca^{2+} in the mitochondrial targeting agent group decreased, and the

Ca²⁺-ATPase increased; the lesion area, collagen and lipid content decreased ($p < 0.05$).

The differentiation of monocytes into macrophages and uptake of modified LDL to produce foam cells is also crucial for the progression of atherosclerosis.¹⁸ We found that mitochondrial targeting agents significantly inhibited atherosclerosis in *ApoE* $-/-$ mice fed a high-fat diet. In addition, mitochondrial targeting agents also inhibited the expression of F4/80 in *ApoE* $-/-$ mice. ICAM-1 is essential for monocyte recruitment. Inflammatory cytokines, such as TNF- α and IL-6, are thought to promote foam cell formation. The silencing of NLRP3 inflammatory bodies leads to the stabilization of atherosclerotic plaques. We observed that the expression of TNF- α , IL-6, NLRP3 and ICAM1 decreased after treatment with mitochondrial targeting agent.

Previous studies have shown that the MAPK/JNK pathway is an important mediator of oxLDL uptake.¹⁹ We found that after the treatment of mitochondrial targeting agents, phospho-p38 and JNK1/2 decreased in atherosclerotic mice. These data indicate that mitochondrial targeting agents can inhibit the development of atherosclerosis and induce the formation of foam cells in *ApoE* $-/-$ mice. The inhibition of mitochondrial targeting agents on atherosclerotic progression is at least partially mediated by the MAPK/JNK pathway.

The inflammasome triggers inflammation by activating caspase-3 and subsequently maturing inflammatory cytokines and triggering a type of inflammatory cell death called fever.²⁰ After NLRP3 is activated, it interacts with ASC. ASC and NLRP3 together lead to the lysis of procaspase-3 and the activation of caspase-3 in the form of spotted cytoplasmic aggregation. We observed that mitochondrial targeting agent treatment reduced the levels of elevated cyt C and cleaved caspase-3 in atherosclerotic mice.

The study has some limitations. The results cannot be extended to other pathological stages of atherosclerosis. It is necessary to further study the role of mitochondrial targeting agents in the formation of advanced plaques.

In conclusion, mitochondrial targeting agents inhibit the activation of the MAPK/JNK pathway by suppressing mitochondrial calcium transport and calcium-induced membrane permeability change, inhibit foam cell formation and alleviate atherosclerosis. More studies are needed to confirm our findings and further explore the role of mitochondrial targeting agents in animal models.

Contributors SC, JW, LZ and HX contributed to the conception and design of the study; SC, JW and LZ performed the experiments, collected and analyzed data; SC and JW wrote the manuscript; all authors reviewed and approved the final version of the manuscript.

Funding The authors have not declared a specific grant for this research from any funding agency in the public, commercial or not-for-profit sectors.

Competing interests None declared.

Patient consent for publication Not required.

Ethics approval All animal experiments were conducted in accordance with the 'Guidelines for the Care and Use of Laboratory Animals' by the National

Institutes of Health and were approved by the hospital animal research ethics review committee.

Provenance and peer review Not commissioned; externally peer reviewed.

Data availability statement Data are available upon reasonable request.

Supplemental material This content has been supplied by the author(s). It has not been vetted by BMJ Publishing Group Limited (BMJ) and may not have been peer-reviewed. Any opinions or recommendations discussed are solely those of the author(s) and are not endorsed by BMJ. BMJ disclaims all liability and responsibility arising from any reliance placed on the content. Where the content includes any translated material, BMJ does not warrant the accuracy and reliability of the translations (including but not limited to local regulations, clinical guidelines, terminology, drug names and drug dosages), and is not responsible for any error and/or omissions arising from translation and adaptation or otherwise.

ORCID iD

Hao Xia <http://orcid.org/0000-0002-8985-3899>

REFERENCES

- 1 Tyrrell DJ, Blin MG, Song J, *et al*. Age-Associated mitochondrial dysfunction accelerates atherogenesis. *Circ Res* 2020;126:298–314.
- 2 Ro S-H, Jang Y, Bae J, *et al*. Autophagy in adipocyte browning: emerging drug target for intervention in obesity. *Front Physiol* 2019;10:22.
- 3 Jin U, Park SJ, Park SM. Cholesterol metabolism in the brain and its association with Parkinson's disease. *Exp Neurol* 2019;28:554–67.
- 4 Gallagher H, Williams JO, Ferekidis N, *et al*. Dihomo- γ -linolenic acid inhibits several key cellular processes associated with atherosclerosis. *Biochim Biophys Acta Mol Basis Dis* 2019;1865:2538–50.
- 5 Wu J, Zeng Z, Zhang W, *et al*. Emerging role of SIRT3 in mitochondrial dysfunction and cardiovascular diseases. *Free Radic Res* 2019;53:139–49.
- 6 Onat Ul, Yildirim AD, Tufanli Özlem, *et al*. Intercepting the lipid-induced integrated stress response reduces atherosclerosis. *J Am Coll Cardiol* 2019;73:1149–69.
- 7 Salerno AG, Rentz T, Dorighello GG, *et al*. Lack of mitochondrial NAD(P)⁺-transhydrogenase expression in macrophages exacerbates atherosclerosis in hypercholesterolemic mice. *Biochem J* 2019;476:3769–89.
- 8 Zakirov FH, Zhang D, Grechko AV, *et al*. Lipid-based gene delivery to macrophage mitochondria for atherosclerosis therapy. *Pharmacol Res Perspect* 2020;8:e00584.
- 9 Nomura M, Liu J, Yu Z-X, *et al*. Macrophage fatty acid oxidation inhibits atherosclerosis progression. *J Mol Cell Cardiol* 2019;127:270–6.
- 10 Oliveira HCF, Vercesi AE. Mitochondrial bioenergetics and redox dysfunctions in hypercholesterolemia and atherosclerosis. *Mol Aspects Med* 2020;71:100840.
- 11 Peng W, Cai G, Xia Y, *et al*. Mitochondrial dysfunction in atherosclerosis. *DNA Cell Biol* 2019;38:597–606.
- 12 Chen Y, Yang M, Huang W, *et al*. Mitochondrial metabolic reprogramming by CD36 signaling drives macrophage inflammatory responses. *Circ Res* 2019;125:1087–102.
- 13 Yang X, Pan W, Xu G, *et al*. Mitophagy: a crucial modulator in the pathogenesis of chronic diseases. *Clin Chim Acta* 2020;502:245–54.
- 14 Sun X, Seidman JS, Zhao P, *et al*. Neutralization of oxidized phospholipids ameliorates non-alcoholic steatohepatitis. *Cell Metab* 2020;31:189–206.
- 15 Yuan T, Yang T, Chen H, *et al*. New insights into oxidative stress and inflammation during diabetes mellitus-accelerated atherosclerosis. *Redox Biol* 2019;20:247–60.
- 16 Daenen K, Andries A, Mekahli D, *et al*. Oxidative stress in chronic kidney disease. *Pediatr Nephrol* 2019;34:975–91.
- 17 Bai X-L, Deng X-L, Wu G-J, *et al*. Rhodiola and salidroside in the treatment of metabolic disorders. *Mini Rev Med Chem* 2019;19:1611–26.
- 18 Glanz VY, Sobenin IA, Grechko AV. The role of mitochondria in cardiovascular diseases related to atherosclerosis. *Front Biosci (Elite Ed)* 2020;12:102–12.
- 19 Chen Q, Lv J, Yang W, *et al*. Targeted inhibition of STAT3 as a potential treatment strategy for atherosclerosis. *Theranostics* 2019;9:6424–42.
- 20 Negre-Salvayre A, Guerby P, Gayral S, *et al*. Role of reactive oxygen species in atherosclerosis: lessons from murine genetic models. *Free Radic Biol Med* 2020;149:8–22.